We are IntechOpen,
the world's leading publisher of
Open Access books
Built by scientists, for scientists

4,800
Open access books available

122,000
International authors and editors

135M
Downloads

Our authors are among the

154
Countries delivered to

TOP 1%
most cited scientists

12.2%
Contributors from top 500 universities

CLARIVATE ANALYTICS

BOOK CITATION INDEX

INDEXED

WEB OF SCIENCE™

Selection of our books indexed in the Book Citation Index
in Web of Science™ Core Collection (BKCI)

Interested in publishing with us?
Contact book.department@intechopen.com

Numbers displayed above are based on latest data collected.
For more information visit www.intechopen.com

Characterization of Ferroelectric Materials by Photopyroelectric Method

Dadarlat Dorin[1], Longuemart Stéphane[2] and Hadj Sahraoui Abdelhak[2]
[1]National R&D Institute for Isotopic and Molecular Technologies Cluj-Napoca,
[2]University Lille Nord de France, ULCO, Dunkerque,
[1]Romania
[2]France

1. Introduction

During last decades, the photothermal techniques have been largely applied to the study of thermal and optical properties of condensed matter. Photothermal techniques are based on the same physical principle: the optical energy, absorbed by given material, is partially converted into heat; depending on the way used to measure the quantity of heat and to follow its propagation through the material, several photothermal techniques have been developed (photoacoustic calorimetry, photothermal radiometry, photothermal deflection, thermal lensing, photopyroelectric method) (Tam, 1986). In this chapter we will focus on the simplest one, the photopyroelectric calorimetry and its applications concerning the investigation of some thermal and electrical properties of ferroelectric materials.

The photopyroelectric (PPE) detection was introduced in 1984, as a powerful tool for high-resolution measurement of thermal properties of materials (Coufal, 1984; Mandelis, 1984). The pyroelectric effect consists in the induction of spontaneous polarization in a noncentrosymmetric, piezoelectric crystal, as a result of temperature change in the crystal. Single crystals as $LiTaO_3$ and TGS, ceramics as PZT or polymers as PVDF were used as pyroelectric sensors, for the main purpose of measuring temperature variations. In principle, in the PPE method, the temperature variation of a sample exposed to a modulated radiation is measured with a pyroelectric sensor, situated in intimate thermal contact with the sample (Mandelis & Zver, 1985; Chirtoc & Mihailescu, 1989). The main advantages of this technique were found to be its simplicity, high sensitivity, non-destructive character and adaptability to practical restrictions imposed by the experimental requirements.

From theoretical point of view, in the most general case, the complex PPE signal depends on all optical and thermal parameters of the different layers of the detection cell. A large effort was dedicated in the last decades to simplify the mathematical expression of the PPE signal. As a final result, several particular cases were obtained, in which the information is contained both in the amplitude and phase of the PPE signal (Mandelis & Zver, 1985; Chirtoc & Mihailescu, 1989); the amplitude and phase depend in these cases on one or, in a simple way, on two of the sample's related thermal parameters.

The thermal parameters resulting directly from PPE measurements are usually the thermal diffusivity and effusivity. It is well known that the four thermal parameters, the static volume specific heat, C, and the dynamic thermal diffusivity, α, conductivity, k, and effusivity, e, are

connected by two relationships, $k=C\alpha$ and $e=(Ck)^{1/2}$; in conclusion, only two are independent. It is important to note that the PPE calorimetry is (at the authors knowledge) the only technique able to give *in one measurement* the value of two (in fact all four) thermal parameters.

Consequently, it is obvious that the PPE method is suitable not only to characterize from thermal point of view a large class of solids and liquids, but also to study processes associated with the change of the thermal parameters as a function of temperature (phase transitions, for example), composition (chemical reactions), time (hygroscopicity), etc.

A particular application of the PPE calorimetry is the characterization of the ferroelectric materials. The application is particular in this case because many ferroelectric materials are in the same time pyroelectric materials. Consequently the investigated ferroelectric specimen can be inserted in the PPE detection cell, both as sample or (sometimes) as pyroelectric sensor, offering additional possibilities for thermal characterization.

This chapter makes a brief summary of the theoretical and experimental possibilities offered by the PPE calorimetry in thermal characterization of some ferroelectric materials; the advantages and the limitations of the technique, as well as a comparison with other techniques are presented.

2. Development of the PPE theoretical aspects concerning the thermal characterization of ferroelectric materials

From theoretical point of view, there are two PPE detection configurations, "back" and "front", mainly applied for calorimetric purposes. In the back (BPPE) configuration, a modulated light impinges on the front surface of a sample, and a pyroelectric sensor, situated in good thermal contact with the sample's rear side, measures the heat developed in the sample due to the absorption of radiation. In the front (FPPE) configuration, the radiation impinges on the front surface of the sensor, and the sample, in good thermal contact with its rear side, acts as a heat sink (Mandelis & Zver, 1985; Chirtoc & Mihailescu, 1989). The geometry of the BPPE and FPPE configurations is presented in Fig.2.1.
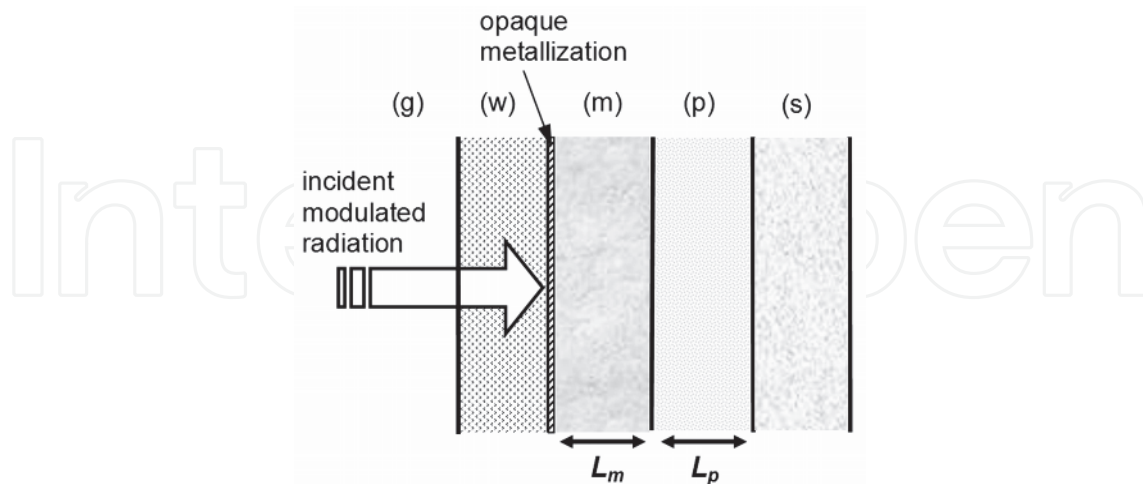

Fig. 2.1 Schematic diagram of the PPE detection cell: (g) – air, (w) – window, (m) – material, (p) – pyroelectric sensor, (s) – substrate.

In the BPPE configuration the ferroelectric sample is represented by the "material" (m) layer; in the FPPE configuration, the "material" layer is missing, and the investigated material is the pyroelectric sensor itself.

2.1 Ferroelectric material inserted as sample in the detection cell ("back" detection configuration)

With the additional simplifying assumptions that the window and substrate are thermally thick, the air and window are optically transparent and the incident radiation is absorbed only at the window-material interface (by a thin opaque layer), the PPE voltage is given by (Delenclos et al., 2002):

$$V = \frac{2V_0 \exp(-\sigma_m L_m)}{(b_{wm}+1)(b_{mp}+1)} \times$$
$$\frac{\exp(-\sigma_p L_p) + R_{sp}\exp(-\sigma_p L_p) - (1+R_{sp})}{\exp(-\sigma_p L_p) - R_{sp}R_{mp}\exp(-\sigma_p L_p) + (R_{mp}\exp(\sigma_p L_p) - R_{sp}\exp(-\sigma_p L_p))R_{wm}(-2\sigma_m L_m)} \tag{2.1}$$

where

$$R_{jk} = (b_{jk}-1)/(b_{jk}+1); \quad b_{jk} = e_j/e_k; \quad \sigma_j = (1+i)a_j; \quad \mu = (2\alpha/\omega)^{1/2} \tag{2.2}$$

In Eq. (2.1), V_0 is an instrumental factor, R_{jk} represents the reflection coefficient of the thermal wave at the 'jk' interface, ω is the angular chopping frequency and σ and a are the complex thermal diffusion coefficient and the reciprocal of the thermal diffusion length ($a = 1/\mu$), respectively. In order to eliminate V_0, a normalization of the signal is necessary, the best reference signal being obtained by the direct illumination of the empty sensor. The obtained normalized signal is:

$$V_n(f) = \frac{2(b_{gp}+1)}{(b_{wm}+1)(b_{mp}+1)}\exp(-\sigma_m L_m)P(f) \tag{2.3}$$

where

$$P(f) = \frac{1 - R_{sp}R_{gp}\exp(-2\sigma_p L_p)}{1 - R_{sp}R_{mp}\exp(-2\sigma_p L_p) + [R_{mp} - R_{sp}\exp(-2\sigma_p L_p)]R_{wm}\exp(-2\sigma_m L_m)} \tag{2.4}$$

If we work in the thermally thick regime for the sensor ($L_p \gg \mu_p$) and we extract the phase and the amplitude from Eq. (2.3), we get for the phase:

$$\Theta = -\arctan\left(\frac{\tan(a_m L_m)[1 + R\exp(-2a_m L_m)]}{1 - R\exp(-2a_m L_m)}\right) \tag{2.5}$$

with $R = R_{mw}R_{mp}$, and for the amplitude:

$$\ln V_n = \ln\frac{2(b_{gp}+1)}{(b_{wm}+1)(b_{mp}+1)}) - a_m L_m \tag{2.6}$$

An analysis of Eq. (2.5) indicates that the sample's thermal diffusivity (contained in a_m) can be directly measured by performing a frequency scan of the phase of the PPE signal. The most suitable particular case seems to be the thermally thick regime for the sample, ($L_m \gg \mu_m$), when Eqs. (2.5) and (2.6) reduce to:

$$V_n = V_0 \frac{\exp\left[-L_m\left(\omega/2\alpha_m\right)^{1/2}\right]}{e_p + e_m};$$ (2.7)

$$\Theta = \Theta_0 - L_m\left(\frac{\omega}{2\alpha_m}\right)^{1/2}.$$ (2.8)

Inserting the value of the thermal diffusivity from Eq. (2.8) in Eq. (2.7) we obtain the value of the thermal effusivity, and, using then the well known relationships between the thermal parameters, we get the values of the remaining two thermal parameters, volume specific heat and thermal conductivity.

2.2 Ferroelectric material inserted as sensor in the detection cell ("front" detection configuration)

In the previous paragraph, a pyroelectric sensor was placed in thermal contact with the studied ferroelectric sample. However, as mentioned before, it is possible to extract information on the pyroelectric material itself. The configuration is in this case simpler, being reduced to a three layers model: front medium-air, pyro(ferro)electric material (p) with opaque electrodes, and a substrate (s) in good thermal contact with the pyroelectric sensor (Fig. 2.2.).
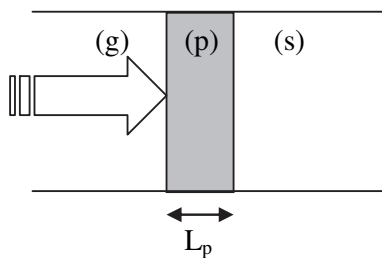

Fig. 2.2 Schematic diagram of the PPE detection cell: (g) – air, (p) – pyroelectric sample, (s) – substrate

If we consider the front medium (g) and the substrate (s) as semi-infinite ($L_g \gg \mu_g$ and $L_s \gg \mu_s$) the PPE voltage is given by :

$$V = \frac{V_0}{b_{gp}+1}\frac{1-\exp(-\sigma_p L_p) + R_{sp}[\exp(-2\sigma_p L_p)-\exp(-\sigma_p L_p)]}{1-R_{gp}R_{sp}\exp(-2\sigma_p L_p)}.$$ (2.9)

Considering frequencies for which the quantity $\exp(-2\sigma_p L_p)$ can be neglected, the signal expression reduces to:

$$V = \frac{V_0}{b_{gp}+1}[1-(1+R_{sp})\exp(-\sigma_p L_p)].$$ (2.10)

The signal can be normalized by the one obtained with empty sensor, leading to:

$$V_n = 1-(1+R_{sp})\exp(-\sigma_p L_p).$$ (2.11)

The amplitude and the phase of the normalized complex signal are then expressed as:

$$\Theta = \arctan \frac{(1+R_{sp})\exp(-a_p L_p)\sin(a_p L_p)}{1-(1+R_{sp})\exp(-a_p L_p)\cos(a_p L_p)} ; \qquad (2.12)$$

$$|V_n| = \sqrt{[(1+R_{sp})\exp(-a_p L_p)\sin(a_p L_p)]^2 + [1-(1+R_{sp})\exp(-a_p L_p)\cos(a_p L_p)]^2} . \quad (2.13)$$

In conclusion to this sub-section, the thermal diffusivity of the ferroelectric layer can be extracted carrying out a frequency scan of the complex PPE signal. Concerning the normalized phase (Eq. (2.12)), it has an oscillating behaviour with zero crossing at frequencies for which $a_p L_p$ is a multiple of π. The values of these frequencies allow a direct determination of the thermal diffusivity of the ferroelectric material, providing its thickness is known and independently on the type of substrate. The value of the thermal diffusivity can be then used in the equation of the normalized amplitude or phase in order to obtain the thermal effusivity of the pyro(ferro)electric layer (providing the effusivity of the substrate is known). In addition to the thermal parameters, it is also possible to extract the temperature dependence of the pyroelectric coefficient γ of the pyroelectric from the instrumental factor V_0. In current mode, it is expressed as:

$$V_0 = -\frac{\gamma I_0 Z_f}{2L_p C_p}, \qquad (2.14)$$

with I_0 the intensity of the modulated light source and Z_f the feedback complex impedance of the current preamplifier. The normalized signal amplitude's variation with temperature is then proportional to γ / C_p.

3. Instrumentation

3.1 Experimental set-up
The experimental set-up for PPE calorimetry contains some typical components (Fig. 3.1).
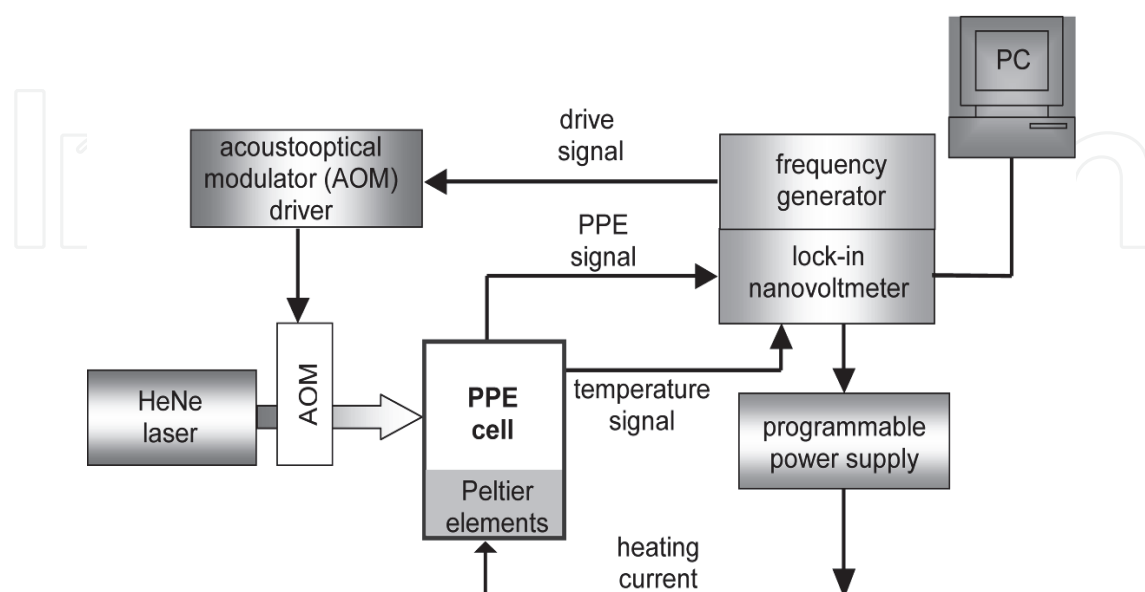

Fig. 3.1 Typical experimental set-up for PPE calorimetry.

The radiation source, usually a laser, is modulated by an acousto-optical modulator or an electro-mechanical chopper. The PPE signal is processed with a lock-in amplifier. A computer with adequate software is used for data acquisition. When performing temperature scans (phase transition investigations, for example), a thermostat, provided with Peltier elements (Jalink et al., 1996), or "cold finger" refrigerator systems (Chirtoc et al., 2009) with additional equipment (programmable power supply, electronic thermometer, etc.) for temperature control, is included in the set-up.

3.2 Detection cells

In the following we will describe some typical detection cells used for PPE calorimetry of ferroelectric materials. All presented cells can operate at room temperature or can be used for temperature scans.

3.2.1 Cold-finger cell

The cold-finger concept (Fig. 3.2) allows investigations at temperatures both below and above the ambient. The cell is provided with two windows, for investigations in both BPPE and FPPE configurations. In principle, the copper bar transmits the temperature to the sample – one extremity of the bar can be cooled down by using liquid nitrogen, or heated up electrically, with a resistive coil. The role of the 0.1 mm thick steel cylinder is to keep the cell (excepting the copper bar) at room temperature. Depending on the operating temperature, one can make vacuum inside the cell or introduce dry atmosphere. The temperature of the sample is measured with a diode, glued with silicon grease to the cold finger, in the vicinity of the sample.
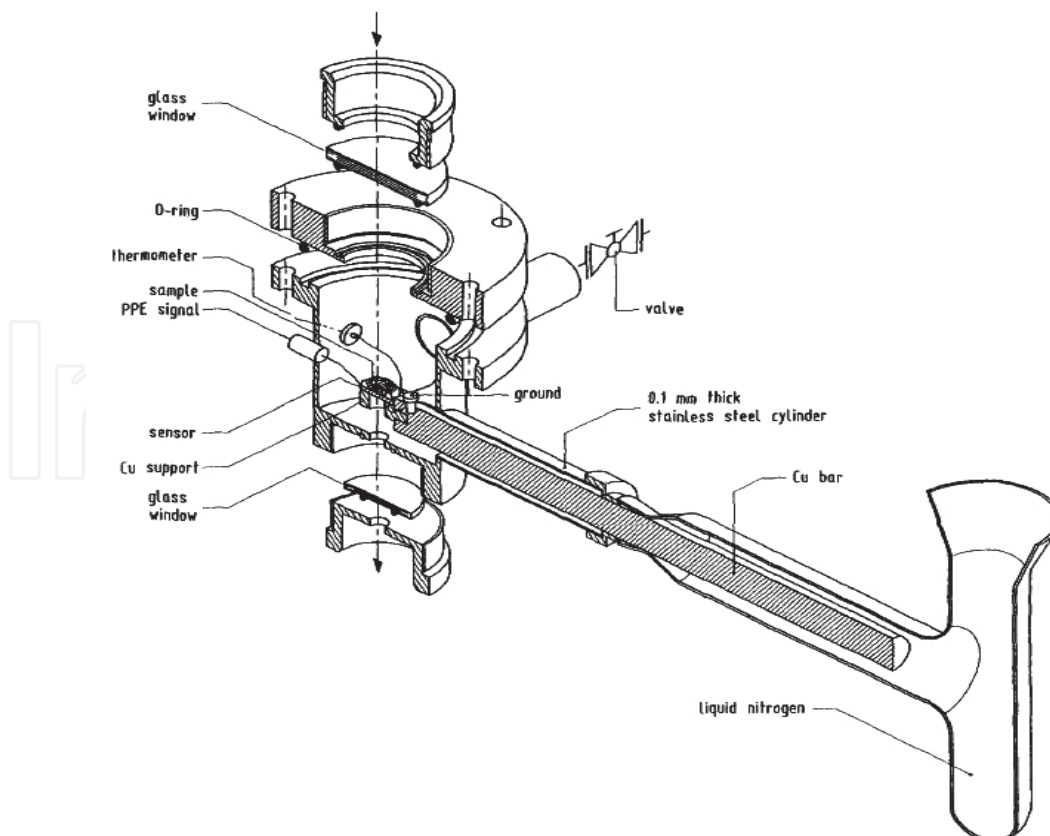

Fig. 3.2 Cold finger refrigerator system

3.2.2 Detection cell provided with Peltier elements

The design of the PPE detection cell equipped with Peltier elements is presented in Fig. 3.3. One face of one of the two Peltier elements (electrically connected in parallel) is thermally connected to a thermostat (liquid flux from a thermostatic bath). The opposite face of the second Peltier element is in thermal contact with an inside-chamber that accommodates the sample-sensor assembly. Temperature feed-back is achieved with a thermistor placed close to the sensor. Computer-controlled temperature scans with positive/negative rates (heating/cooling) are possible.
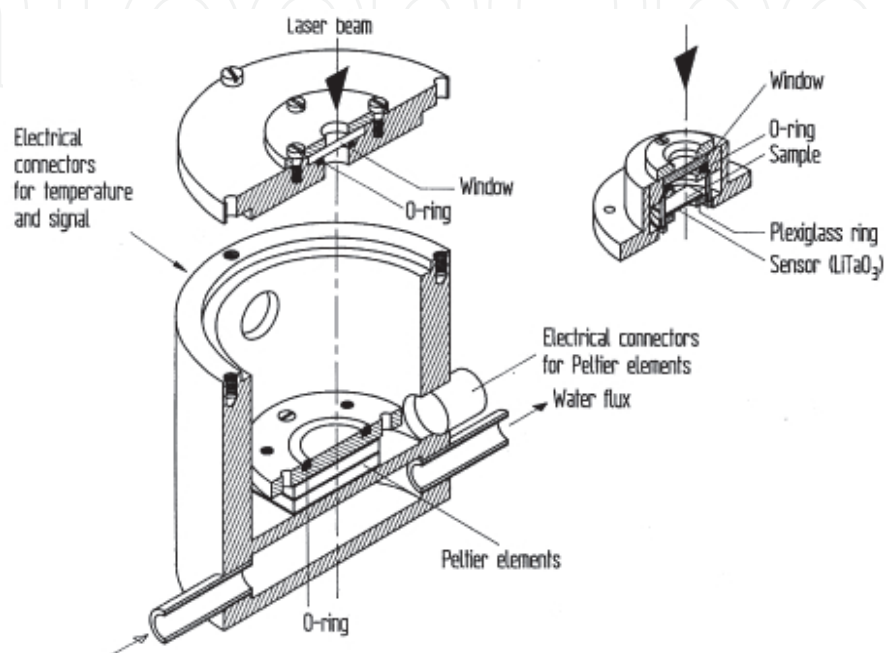

Fig. 3.3 PPE detection cell provided with Peltier elements

3.2.3 Application of an electric field to the sample

The electrical and thermal properties of a ferroelectric material usually depend on an external electric field. The investigation of these properties under external electric field requires some adaptation of the detection cell. Basically, as mentioned above, two cases must be considered: either the ferroelectric sample is in thermal contact with a pyroelectric sensor, either the sample is the sensor itself.

In the first case, in order to avoid the influence of the electric field on the pyroelectric signal, a special attention must be paid for the ground of the signal: the best alternative is to use one electrode of the sensor as a common ground for both the pyroelectric signal and the external applied voltage (Fig. 3.4).
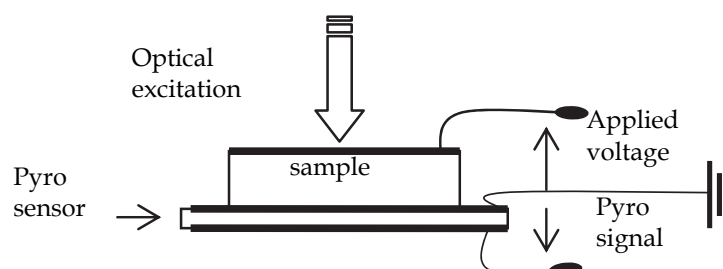

Fig. 3.4 Electrical connections for PPE measurement under electric field.

When the investigated sample is the sensor itself, it is not possible to use the same set-up, because the lock-in amplifier doesn't accept high input voltage. The sample, having usually high impedance, can be inserted in serial inside a circuit constituted of the bias voltage power supply and the lock-in amplifier. In such a way, the input of the lock-in amplifier is not affected by the relative high (tens of volts) applied bias voltage to the sample (Fig. 3.5).
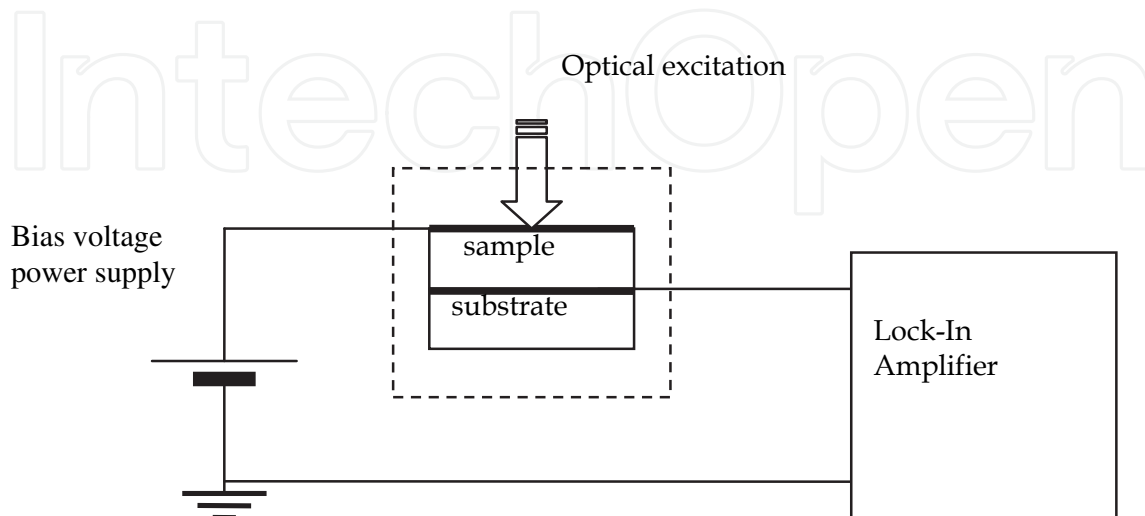

Fig. 3.5 Electrical arrangement for PPE measurement, when applying electric field to the material acting as sensor.

4. Applications

4.1 Investigation of thermal parameters of ferroelectric thin films

For most of the applications concerning the ferroelectric materials, the knowledge of their thermal parameters is necessary because they are relevant for evaluating the figure of merit of a IR sensor (Whatmore, 1986), or a pyroelectric accelerator (Fullem and Danon, 2009) for instance. When used as a sensor in a PPE experiment, the knowledge of these parameters is crucial, because all other measured properties depend of these values (Bentefour et al., 2003). Moreover, it has been shown (Nakamura et al., 2010) that these parameters have slightly different values as a function of the composition/purity of the ferroelectric material.

In the following we consider an opaque ferroelectric material with electrodes perpendicular to the spontaneous polarization, placed in thermal contact with a substrate, the normalized pyroelectric voltage phase and amplitude, resulting from the periodic heating of the material, in the front configuration, is given by the equation (2.12) and (2.13). In practice, several approaches are possible for extracting the thermal parameters of the pyroelectric sensor from the experimental data. We will present here the results obtained on a largely used pyro(ferro)electric sensor: $LiTaO_3$ single crystal.

4.1.1 Thermal parameters extracted from the phase and amplitude, at a given temperature

The behaviour of the normalized phase and amplitude of the PPE signal, as a function of frequency, obtained for a $510 \mu m$ thick $LiTaO_3$ single crystal is plotted in Fig.4.1.
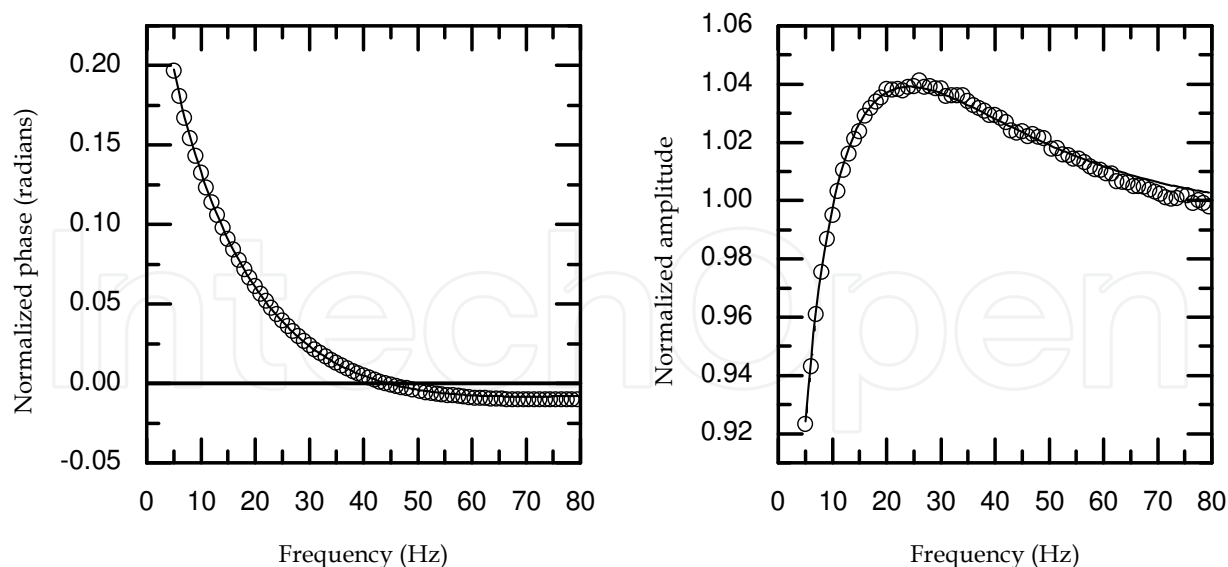
Fig. 4.1 Normalized signal's phase and amplitude obtained with a 510μm thick LiTaO$_3$ film and water as substrate (open circles: experimental data, solid line: best fit).

The phase and amplitude of the signal contain both information about the thermal diffusivity and effusivity of the ferroelectric material. From analytical point of view, the phase goes to zero for a frequency f_0 which verifies the relationship:

$$\frac{L_p \sqrt{f_0}}{\sqrt{\alpha_p}} = \sqrt{\pi} \ .$$ (4.1)

In the experiment described before, f_0 = 44.2 Hz leading to a thermal diffusivity of 1.53 10^{-6} m^2.s^{-1} for LiTaO$_3$. This value can be then introduced in equation (2.12) to extract R_{sp} values and finally the thermal effusivity of LiTaO$_3$:

$$e_p = e_s \left(\frac{1 - R_{sp}}{1 + R_{sp}} \right)$$ (4.2)

Knowing the thermal effusivity of water used as substrate (e_s =1580 W.s$^{1/2}$.m^{-2}.K^{-1}), the average value of the calculated thermal effusivity is e_p = 3603 W.s$^{1/2}$.m^{-2}.K^{-1}. A similar procedure can be adopted to extract the thermal parameters from the amplitude of the signal. The frequency f_1 corresponding to the maximum of the amplitude should verify the relationship (see Eq. 2.13):

$$\frac{L_p \sqrt{f_1}}{\sqrt{\alpha_p}} = \frac{3\sqrt{\pi}}{4}$$ (4.3)

Fig. 4.1 indicates that the amplitude has a maximum for a frequency f_1=25.3Hz, corresponding to a value of 1.56 10^{-6} m^2.s^{-1} for the thermal effusivity of LiTaO$_3$. By inserting this value in Eq. (2.13) one can extract the value of R_{sp} and, using Eq. (4.2), calculate the thermal effusivity of the ferroelectric sample. From data of Fig. 4.1, one finds e_p = 3821 W.s$^{1/2}$.m^{-2}.K^{-1}.

A simple comparison of Eqs. (4.1) and (4.3) indicates that f_1 is theoretically proportional to f_0 by a ratio 16/9. This criterion can be used to estimate the accuracy of the experimental results. For example, in the experiment described before, one finds a ratio of 1.74 between f_1 and f_0, to be compared to the theoretical value of 16/9 (≈ 1.78) . Another way to check for the validity of the experimental results is to combine the phase and the amplitude of the signal. Considering the model described by Eq. (2.11), a plot of the modulus of the complex quantity $(1-V_n)$ as a function of the square root of frequency should display a line whose slope gives the value of the thermal diffusivity of the sample; the extrapolation of the curve to zero frequency leads to the value of the thermal effusivity. Such a calculation has been performed for the experimental data shown in Fig. 4.1 and the result is represented in Fig. 4.2.
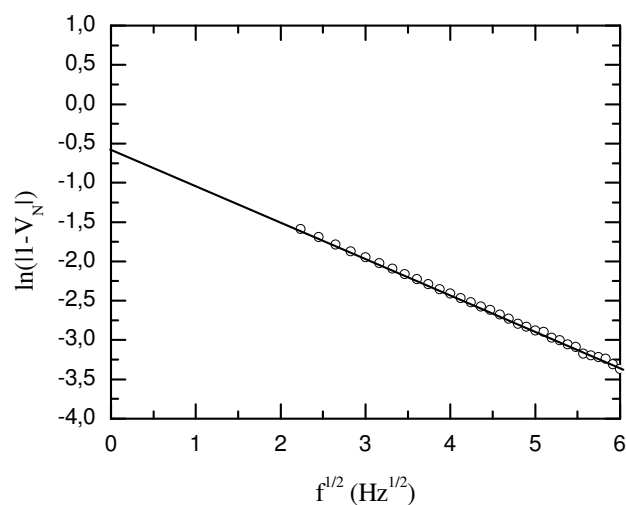

Fig. 4.2 Plot of the logarithm of $|1-V_n|$ as a function of square root of frequency, for data of Fig. 4.1.

Fig. 4.1 indicates that the model is valid for high enough frequencies. The linear fit of the data leads to values of thermal parameters in agreement with previous calculated ones, as reported in table 4.I.

Procedure	Thermal diffusivity ($\times 10^{-6}.m^2.s^{-1}$)	Thermal effusivity ($W.s^{1/2}.m^{-2}.K^{-1}$)
Zero crossing (phase)	1.53	3821
Maximum (amplitude)	1.56	3603
Combination of amplitude and phase (linear fit)	1.58	3886
Non linear fit Phase Amplitude	1.54 1.53	3688 3718

Table 4.I Comparison of values of thermal diffusivity and effusivity, obtained with various procedures, for a 510μm thick LiTaO$_3$ single crystal.

The previous results show that the proposed model allows the determination of the thermal parameters from a frequency scan of the PPE signal generated by the ferroelectric sample

itself. There are several approaches giving similar results (3% to 5% maximum difference for values of thermal diffusivity and effusivity, respectively). However, it should be pointed out that the results obtained with the phase as source of information are often more reliable due to the fact that the amplitude of the signal can be affected by light source's intensity stability as well as by the optical quality of the irradiated surface. Additionally, the frequency dependence of the amplitude around maximum is rather smooth, and the maximum value difficult to be located exactly.

At the end of this section, we have to mention that the theoretical results have been obtained without any hypothesis on the nature of the ferroelectric material used as pyroelectric sensor. The experimental results were obtained on LiTaO$_3$ crystals, but a similar procedure can be carried out for any type of ferroelectric material, as PZT ceramics, polymer films (PVDF, PVDF-TrFE) and even liquid crystal in S$_C$* ferroelectric phase. In the next section this last particular case will be described.

4.1.2 Thermal parameters of a liquid crystal in Sc* ferroelectric phase.

In this subsection the procedure described in the previous section has been extended to the study of a ferroelectric liquid crystal (FLC). In chiral smectic S$_C$* phase of FLCs, molecules are randomly packed in layers and tilted from the layer normal. Each smectic layer possess an in plane spontaneous polarization which is oriented perpendicularly to the molecular tilt. The direction of the tilt plane precesses around an axis perpendicular to the layer planes so that a helicoidal structure of the S$_C$* is formed. In this helicoidal structure, the S$_C$* phase doesn't possess a macroscopic polarization. When it is confined in thin film between two substrates, which are treated so that a planar alignment is imposed on the molecules at the surfaces, as used in surface stabilized FLC (SSFLC) devices (Clark & Lagerwall, 1980; Lagerwall, 1999), the smectic layers stand perpendicular to the surfaces and the helix can be suppressed if the LC film is sufficiently thin. This results in two possible states where the orientation of the molecules in the cell is uniform. The polarization vector in these two states is perpendicular to the substrates but oriented in the opposite direction. In both configurations the S$_C$* film develops a macroscopic polarization, and consequently, a pyroelectric effect of the film can be obtained when it is submitted to a temperature variation. We used the LC film as a pyroelectric sensor and we carried out the procedure described in section 4.1.1 to determine the thermal diffusivity and effusivity of the S$_C$* mesophase.

The ferroelectric liquid crystal (FLC) used in this study was a mixture FELIX 017/000 from Clariant Inc. (Germany). Its phase sequences and transition temperatures (in°C) are: Crystal -26 S$_C$* 70 S$_A$* 75 N* 84.5 I. The sample cell was prepared using a pair of parallel glass substrates. One of the substrates was metallised with gold. It acts as a light absorber and generates a heat wave penetrating into the sample. The other substrate was coated with a transparent electrode of indium-tin oxide in order to control the alignment of the FLC by means of polarized optical microscopy. The gap of the cell was set by a 13 μm thick spacers of PET, and the electrode area was 5 x 5mm². The two plates were spin-coated with PolyVinylAlcohol (PVA) and then rubbed in parallel directions for the FLC alignment. The FLC was inserted by capillary action in the cell in its isotropic phase, then slowly cooled into S$_A$* and S$_C$* in the presence of an AC electric field to achieve uniform alignment of the smectic layers. The sample cell was then observed at room temperature by means of polarized optical microscope. It was found that the LC cell exhibits a uniform texture, and we have not observed any "up" and "down" polarization domains coexistence.

In the previous section, the studied pyroelectric sample was a solid material and the normalizing signal was obtained by using air as substrate. Here, the studied material is fluid (this is the case of the liquid crystal material), the normalizing signal is then obtained using another solid pyroelectric material with air as substrate. In this case the normalized signal is given by:

$$V_n = \frac{K_0}{K_1}(1 - (1 + R_{sp})\exp(-\sigma_p L_p)) \tag{4.4}$$

K_0/K_1 is a real factor independent of the modulation frequency and represents the limit value of the normalized amplitude at high frequency. This factor does not affect the analysis carried out on Eq. (2.11) for the determination of the thermal parameters. The frequency of the zero crossing of the normalized phase (Eq. 3.1) or the frequency corresponding to the normalized amplitude maximum (Eq. 3.3) allows the determination of the absolute value of the thermal diffusivity of the sample. The thermal effusivity can also be calculated from the normalized amplitude once α_p is obtained and the quantity K_0/K_1 is determined from the value of the normalized amplitude at high frequency. The frequency behaviour of the normalized phase of the PPE signal is shown in Fig. 4.3.a

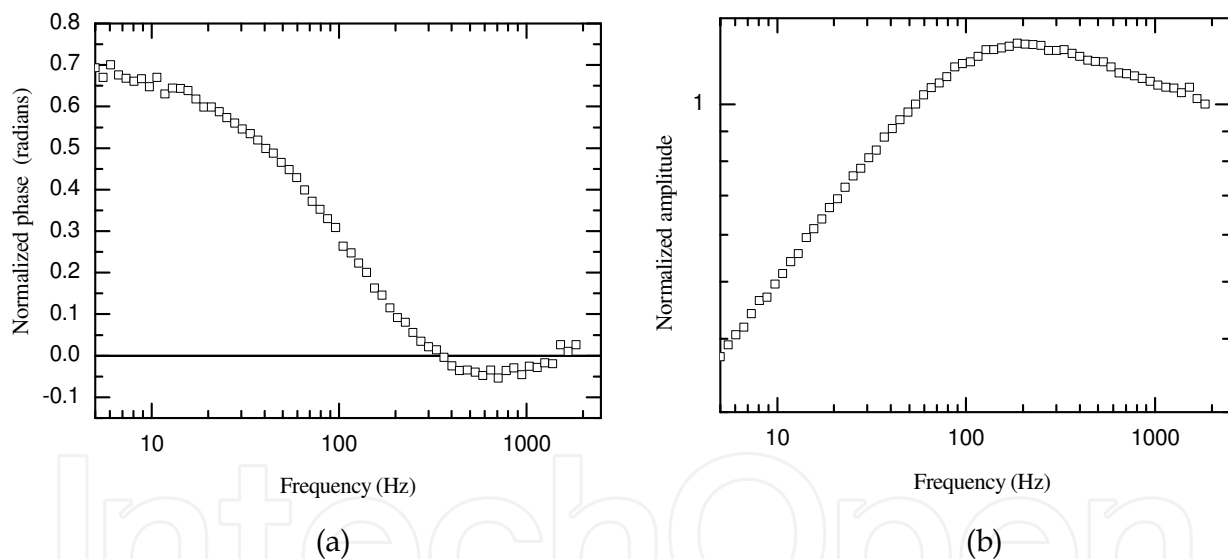(a)   (b)

Fig. 4.3 Experimental frequency behaviour of the normalized phase (a) and the normalized amplitude (b) obtained for the liquid crystal at room temperature, in the S_C* phase.

As expected from the theory, the phase goes to zero, for a frequency $f_0 = 354$ Hz. Once f_0 is determined, equation 4.1 is used to obtain the thermal diffusivity of the ferroelectric liquid-crystal sample. A value of $\alpha_p = 1.90 \ 10^{-8}$ m² s⁻¹ was found.

The normalized amplitude of the PPE signal (Fig. 4.3.b) shows a maximum for the frequency $f_1 = 191$ Hz. The value of α_p calculated by using Eq. (4.3) is $\alpha_p = 1.82 \ 10^{-8}$ m² s⁻¹, denoting that the values of the thermal diffusivity obtained independently from phase and amplitude are in good agreement.

The effusivity e_p is calculated from the signal phase by using Eqs. (2.12) and (4.2) and taking from the literature the value of the thermal effusivity of glass ($e_s = 1503$ Ws$^{1/2}$ m⁻² K⁻¹). The

mean value of e_p is then calculated in a range of frequencies for which the sample is thermally thick; e_p is found to be 340W s$^{1/2}$ m^{-2} K^{-1}.

The same procedure carried out for different temperatures allows for example the investigation on the temperature dependence of the thermal parameters of the smectic S$_C$* phase and near the S$_C$*-S$_A$* transition of FLC materials. However, the use of frequency scans together with temperature scanning procedures can be time consuming when working in the vicinity of critical regions. In the next section, we will introduce a procedure avoiding such frequency scans.

4.1.3 The temperature dependence of the thermal parameters

In the previous section, it has been shown that a frequency scan of the amplitude and/or the phase of the photopyroelectric signal allows the direct measurement of the room temperature values of thermal diffusivity and effusivity of a ferroelectric material and consequently, the calculation of its heat capacity and thermal conductivity. In the following we will describe a procedure useful to study the temperature evolution of these thermal parameters without involving any frequency scan.

Considering the modulus A and the argument ϕ of the complex quantity 1-V_n, and using Eq. (2.11), one has:

$$A = (1 + R_{sp}) \exp(-a_p L_p) \text{ and } \phi = a_p L_p$$

The expression for the thermal diffusivity and thermal effusivity is obtained as a function of A and ϕ as:

$$\alpha_p = \frac{L_p^2 \pi f}{\phi^2} \tag{4.5}$$

$$R_{sp} = \frac{A}{\exp(-\phi)} - 1 \tag{4.6}$$

A and ϕ are calculated from the phase Θ and the amplitude $|V_n|$ of the PPE signal, using the relationship:

$$A = \sqrt{|V_n|^2 + 1 - 2|V_n| \cos \Theta} \tag{4.7}$$

$$\phi = \arctan\left[\frac{|V_n| \sin \Theta}{1 - |V_n| \cos \Theta}\right] \tag{4.8}$$

We have applied this procedure to find the temperature dependence of thermal parameters of a 510μm thick LiTaO$_3$ single crystal, provided with opaque electrodes and using ethylene glycol as substrate. The temperature range was 25°C-70°C. During the experiment, the modulation frequency was 7.2Hz. The signal of the LiTaO$_3$ alone (without substrate) was recorded in the same conditions for normalization purposes. The normalized amplitude and phase are represented in Fig. 4.4. The thermal diffusivity and thermal effusivity, calculated from these data, are displayed in Fig. 4.5.
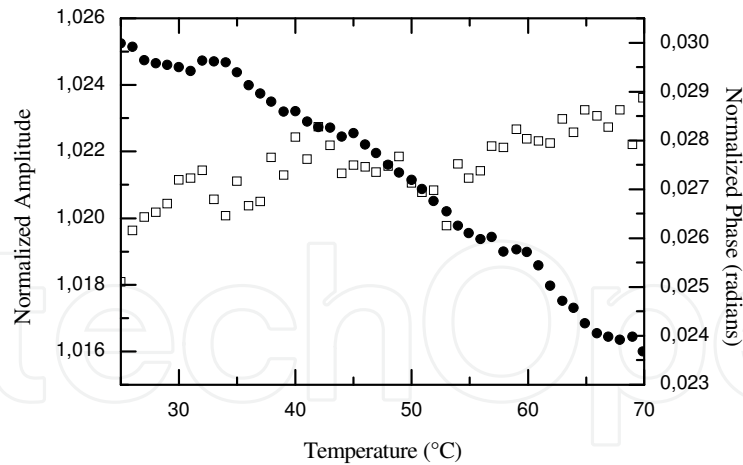
Fig. 4.4 Temperature evolution of the normalized amplitude (empty square) and phase (full circle) of the PPE signal at 7.2Hz of a 510μm thick LiTaO$_3$ single crystal using ethylene glycol as substrate.
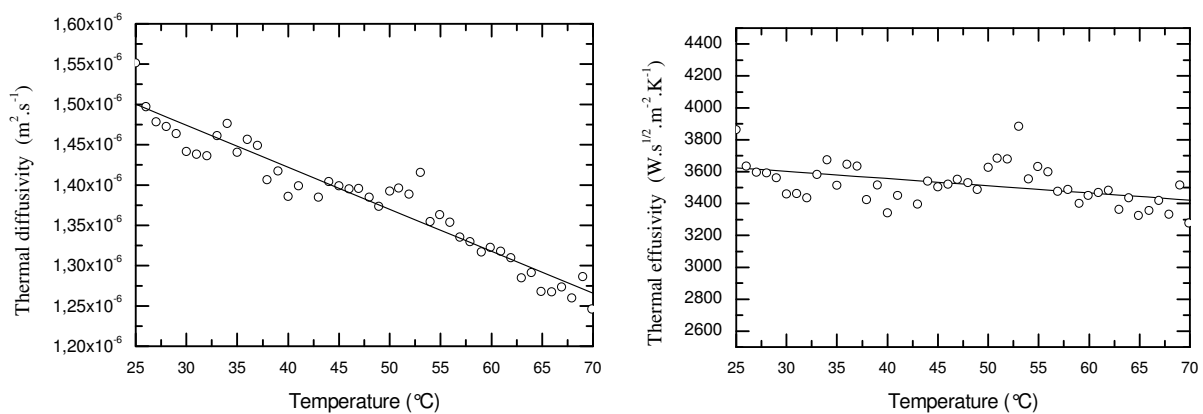

Fig. 4.5 Temperature dependence of the thermal diffusivity and effusivity of LiTaO$_3$ as a function of temperature, calculated from data of Fig. 4.3.

The two others thermal parameters, the volumic heat capacity C_p and the thermal conductivity k_p can then be deduced. The knowledge of C_p allows to extract the temperature dependence of the pyroelectric coefficient γ, from the amplitude of the signal of the sample alone, which is equivalent to the instrumental factor V_0. In the expression of V_0 (Eq. 2.14), only the ration γ/C_p is temperature dependent, thus, multiplying V_0 by the values of C_p and scaling the result to a known value of γ at a given temperature, it is possible to obtain the absolute value of the pyroelectric coefficient as a function of temperature. The results obtained for LiTaO$_3$ are shown in Fig. 4.6 (the value of γ at 25°C was taken from Landolt-Börnstein database (Bhalla and Liu, 1993)).

This subsection was dedicated to experiments in which the combination amplitude-phase of the PPE signal gave information about the room temperature values and temperature dependence of thermal parameters and pyroelectric properties of a ferroelectric material (in position of pyroelectric sensor). Unfortunately, the use of the amplitude of the signal makes the results rather noisy. Such a disadvantage can be avoided by using, when possible, only data from the phase of the signal. In section 4.3.2, a procedure using the signal's phase at two frequencies will be presented, for studies of phase transitions.
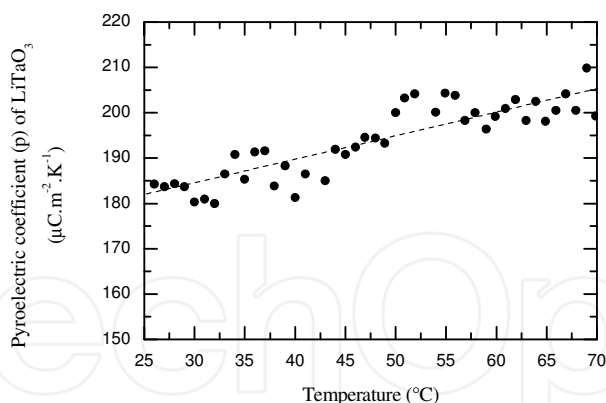
Fig. 4.6 Temperature dependence of the pyroelectric coefficient of LiTaO$_3$ obtained from PPE signal's amplitude.

4.2 PPE detection of phase transitions in ferroelectric materials

As it is well known, phase transitions are processes associated with a breaking of the symmetry of the system. In the case of ferroelectric materials, the ferro-paraelectric phase transition has the polarization as order parameter and, theoretically, it is considered a second order phase transition. Practically, sometimes it was found to be slightly first order (a few amount of latent heat is developed in the process) (del Cerro et al., 1987). For both type of phase transitions (I-st and II-nd order), the second derivatives of some appropriate thermodynamic potential have anomaly at the transition temperature (Curie point for ferroelectric materials). On the other hand, as presented in the theoretical section, the amplitude and phase of the complex PPE signal depend on two (or sometimes one) sample's related thermal parameters. Consequently, it is expected that the PPE technique is suitable to detect both first and second order phase transitions, by measuring the critical anomalies of the thermal parameters.

In time, the PPE technique was applied to detect first (Mandelis et al., 1985) or second (Marinelli et al.,1992) order phase transitions. For second order phase transitions the PPE results were used to calculate the critical exponents of the thermal parameters and to validate the existing theories (Marinelli et al., 1992, Chirtoc and al., 2009). Due to the fact that the PPE technique uses for phase transition investigations the thermal parameters, a wide range of materials belonging to condensed matter, can be listed as investigated specimens: ordinary liquids and liquid mixtures, liquid crystals, liquid, pasty or solid foodstuffs, ferroelectric and magnetic materials, high T$_c$ superconductors, plastics, etc

One of the most important points in making high-temperature-resolution measurements of thermal parameters in the critical region of a phase transition is that the thermal gradients in the investigated sample must be as small as possible. Often, at a phase transition, a strong temperature dependence of the thermal parameters is present when approaching the critical temperature. Thermal gradients tend to smear out this temperature dependence and, sometimes, the phase transition is difficult to be detected. To avoid this effect, it is important to keep the sample in quasi-thermal equilibrium. The measuring techniques, that in most cases are based on the detection of a sample temperature rise, as a response to a heat input, are additional sources of temperature gradients, especially for ac techniques. Accordingly, the techniques involving periodic heating of the sample are preferred, and the PPE technique is among them.

Concerning the ferroelectric materials, Mandelis et al. used for the first time the PPE method for detecting the ferro-paraelectric phase transition in Seignette salt (Mandelis et al., 1985). In the following we will present an application of the PPE technique in detecting the ferroelectric-paraelectric phase transition in a well known ferroelectric crystal, TGS.

4.2.1 TGS as a sample

When inserting a TGS crystal as sample in a PPE detection cell, one has to use the back (BPPE) configuration, with the TGS crystal in the front position (directly irradiated), in intimate thermal contact (through a thin coupling fluid) with a pyroelectric sensor (LiTaO$_3$ or PZT). In experimental conditions of opaque and thermally thick sample and thermally thick sensor, the amplitude, V, and phase, Θ, of the PPE signal are given by the Eqs. (2.7) and (2.8).

An inspection of Eqs.(2.7)-(2.8) leads to the conclusion that it is possible to obtain the temperature behaviour of all four thermal parameters, from one measurement, if we have an isolated value of one thermal parameter (other than thermal diffusivity), to calibrate the amplitude measurement. Consequently, we can obtain the critical behaviour of all static and dynamic thermal parameters around the Curie temperature of a ferroelectric material.

Some important features of Eq. (2.7) should be also stressed:

-   The amplitude of the PPE signal is attenuated by an exponential factor as a$_m$L$_m$ increases;
-   The sensitivity of the signal amplitude to the changes in the thermal diffusivity is given by the ratio:

$$\frac{dV}{V} \bigg/ \frac{d\alpha_m}{\alpha_m} = -\frac{a_m L_m}{2} \tag{4.9}$$

   showing that for $a_m L_m > 2$, a given anomaly in the thermal diffusivity, produces an enhanced signal anomaly;
-   For a given sample, the exponent in Eq. (2.7) can be adjusted by changing the modulation frequency and/or sample's thickness, in order to achieve an optimum trade-off between sensitivity and signal-to-noise ratio.

Based on these theoretical predictions, one can start investigating the ferroelectric-paraelectric phase transition of TGS crystal, by performing a room temperature frequency scan of the phase of the PPE signal, in order to obtain the room temperature value of the thermal diffusivity. A typical result is presented in Fig. 4.7.
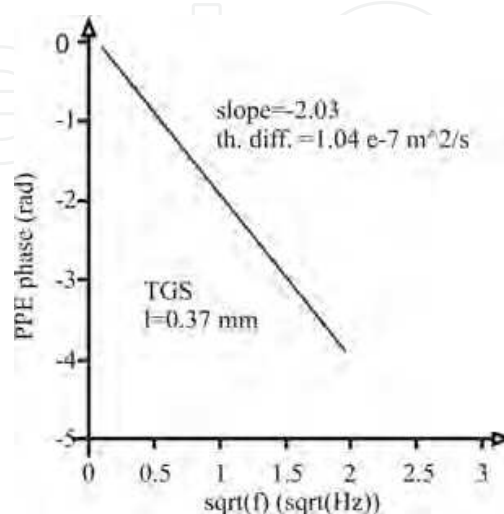

Fig. 4.7 Room temperature frequency scan for the phase of the PPE signal

Typical temperature scans of the amplitude and phase of the PPE signal, in a temperature range including the Curie point of TGS are displayed in Fig.4.8
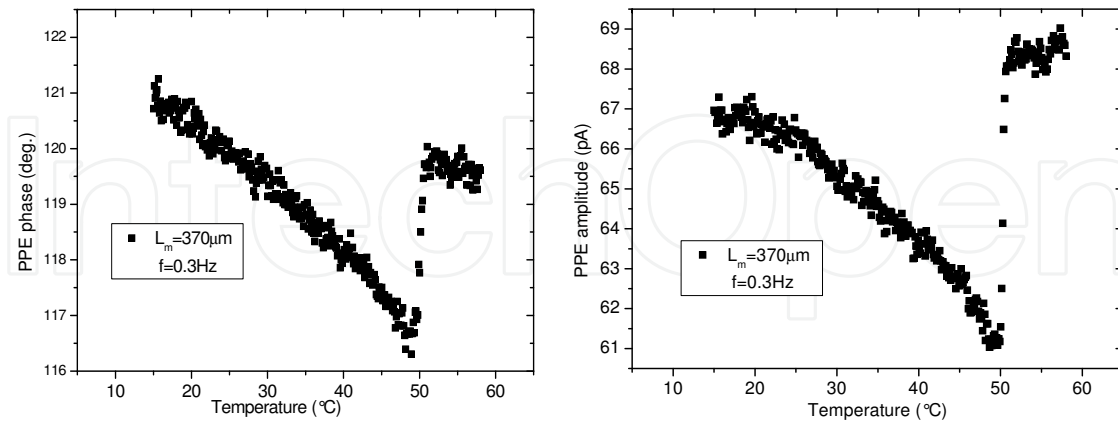

Fig. 4.8 Temperature scan for the phase and the amplitude of the PPE signal

Using Eqs. (2.7)-(2.8), the value of the thermal diffusivity obtained from the slope of the curve in Fig.4.7, and the value of the thermal conductivity from del Cerro et al., 1987, one gets the critical behaviour of all four thermal parameters (Fig.4.9)
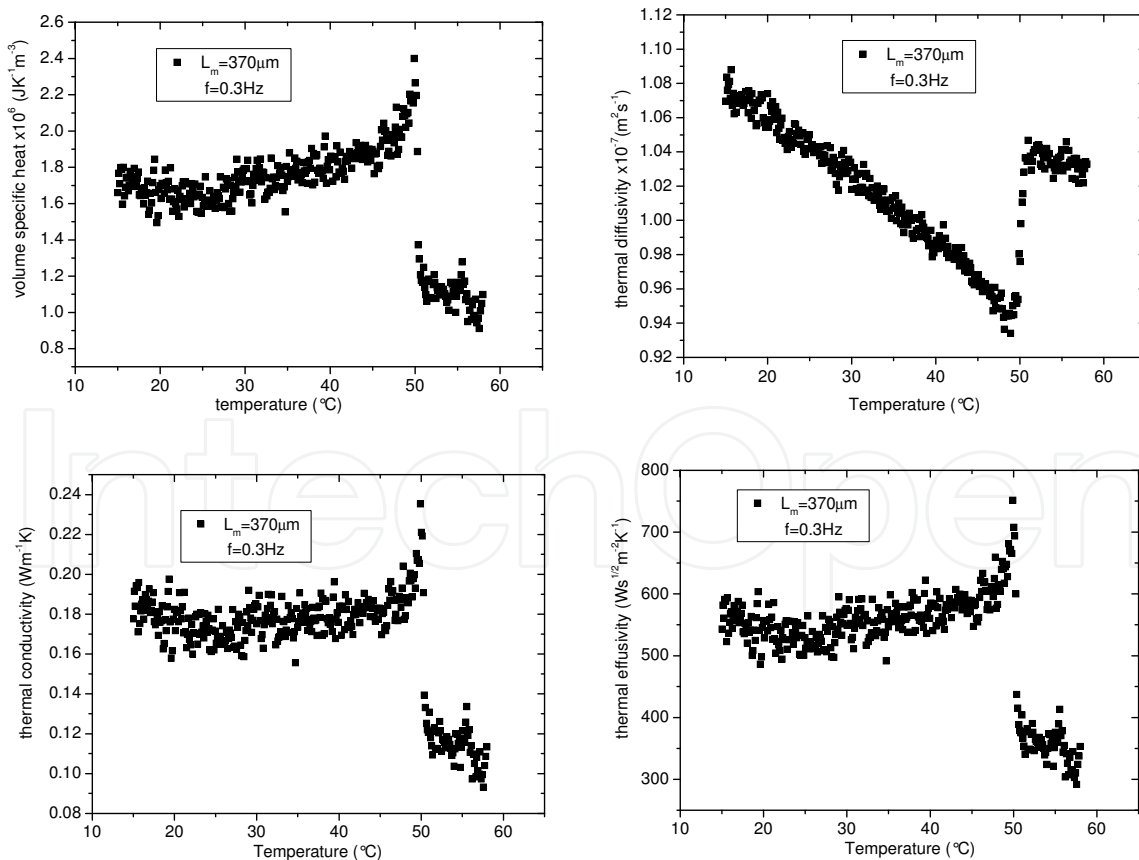

Fig. 4.9 Temperature behaviour of the volume specific heat, thermal diffusivity, conductivity and effusivity of TGS around the Curie point

Some technical details concerning the experiment are: TGS single crystal, 370μm thick, pyroelectric sensor LiTaO$_3$, 300μm thick, chopping frequency for the temperature scan f = 0.3 Hz.

As mentioned above, one of the most important features concerning Eq. (2.7) is the possibility of enhancing the critical anomaly of the thermal diffusivity, by a proper handling of the chopping frequency and sample's thickness.

Such an example, for a TGS crystal with two different thicknesses (230 μm and 500 μm), investigated at different frequencies (6Hz and 25Hz) is displayed in Fig. 4.10. In this experiment, the pyroelectric sensor was a 1mm thick PZT ceramic.
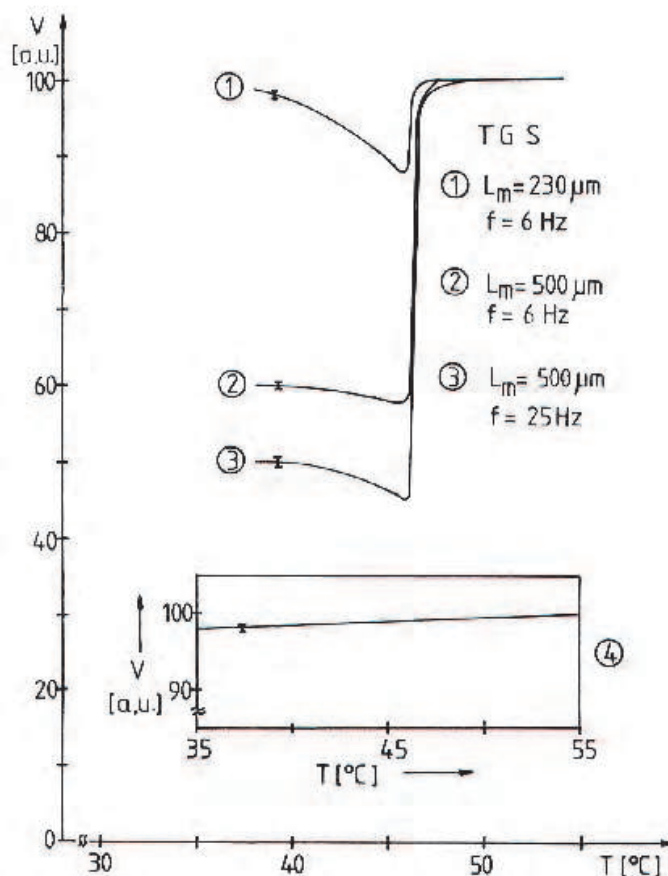
Fig. 4.10 Normalized PPE amplitude as a function of temperature for two TGS single crystals and for two different chopping frequencies (different thermal diffusion length)

Fig. 4.10. indicates that the critical anomaly of the PPE amplitude, $\Delta V/V$, increases from 0.14 up to 1.22 with increasing exponent in Eq. (2.7), for the same critical anomaly (about 0.2 jump in the specific heat – (del Cerro et al., 1987)). This fact supports the suitability of the method for investigations of phase transitions with small critical anomalies of the thermal parameters.

4.2.2 TGS as a pyroelectric sensor

This configuration is based on the information contained in the phase of the FPPE signal and collected from a ferroelectric material, used as pyroelectric sensor in the PPE detection cell.

As presented in the theoretical section, the normalized phase of the FPPE signal, for a detection cell composed by three layers - air, pyroelectric sensor and substrate - is given by:

$$\Theta = \arctan\frac{(1+R_{sp})\exp(-a_pL_p)\sin(a_pL_p)}{1-(1+R_{sp})\exp(-a_pL_p)\cos(a_pL_p)} \tag{4.10}$$

Eq. (4.10) is valid for opaque pyroelectric sensor and for thermally thick substrate. The normalization signal was obtained with empty, directly irradiated sensor. When performing measurements at two different chopping frequencies we obtain:

$$\frac{\tan(\Theta_1)}{\tan(\Theta_2)}=\frac{\exp(-L_p a_{p1})[\cos(L_p a_{p1})+\sin(L_p a_{p1})\tan(\Theta_1)]}{\exp(-L_p a_{p2})[\cos(L_p a_{p2})+\sin(L_p a_{p2})\tan(\Theta_2)]} \tag{4.11}$$

with $a_{p1,2} = (\pi f_{1,2}/a_p)^{1/2}$. Eq. (4.11) indicates that one can obtain the thermal diffusivity of the pyroelectric material, used as sensor in the detection cell, by performing two measurements at two different chopping frequencies, providing the geometrical thickness of the sensor is known.

Typical results, obtained for the phase of the PPE signal for a 500 μm thick TGS single crystal, with silicon oil as substrate (together with the normalization signal - directly irradiated empty sensor) are displayed in Fig. (4.11). An external electric field of 6 kV/m was additionally applied.
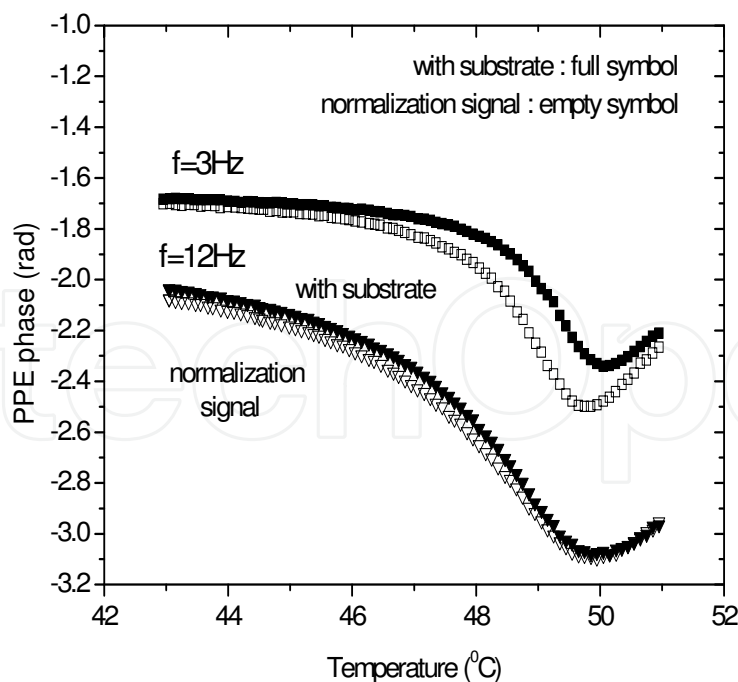

Fig. 4.11 Temperature scans of the phase of the PPE signal, for a 500μm thick TGS single crystal, around the ferroelectric Curie temperature, for 3Hz and 12Hz chopping frequencies, and an external electric field of 6kV/m.
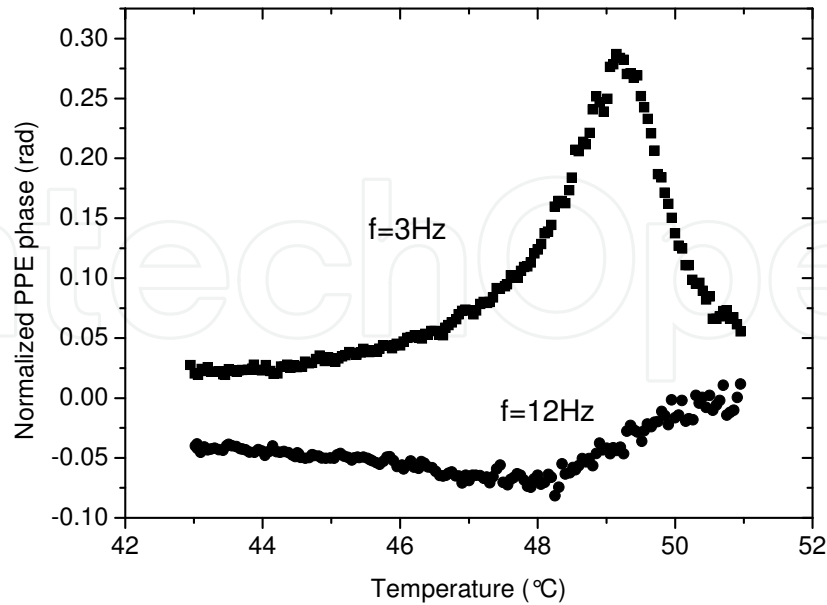
Fig.4.12 Same as Fig.4.11, but for the normalized phase.

Fig. 4.12 presents the normalized phases of the PPE signal for the two frequencies. The critical behaviour of the thermal diffusivity for three values of the external electric field, as obtained from Eq.(4.11), is displayed in Fig. 4.13.
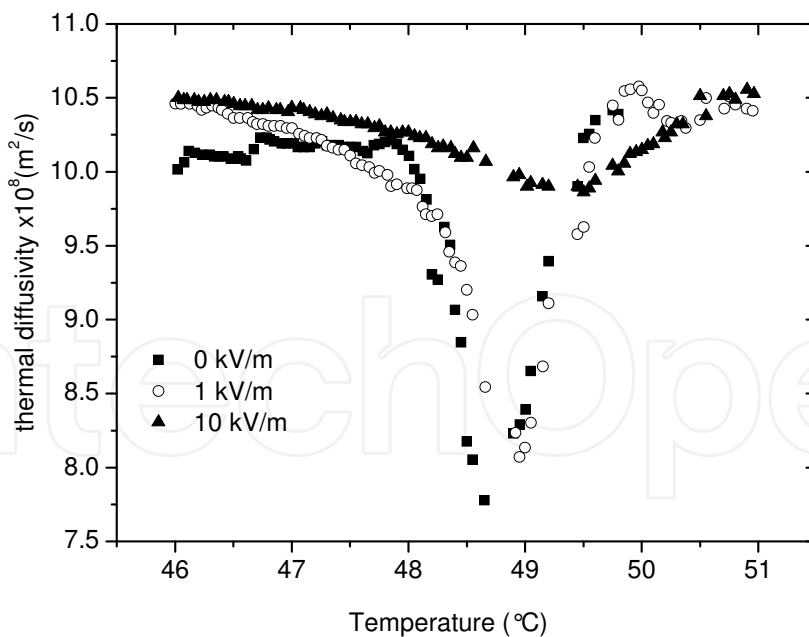

Fig. 4.13 Critical behaviour of the thermal diffusivity of TGS for 0 kV/m (squares); 1 kV/m (circles) and 10 kV/m (triangles).

Fig. 4.13 displays a typical behavior (critical slowing down) of thermal diffusivity for a second order phase transition. The external electric field has the well known influence on the phase transition: it increases the Curie temperature and enlarges the critical region. The

values of the Curie points are in good agreement with those obtained from the direct measurement of the PPE amplitude (Fig. 4.14).
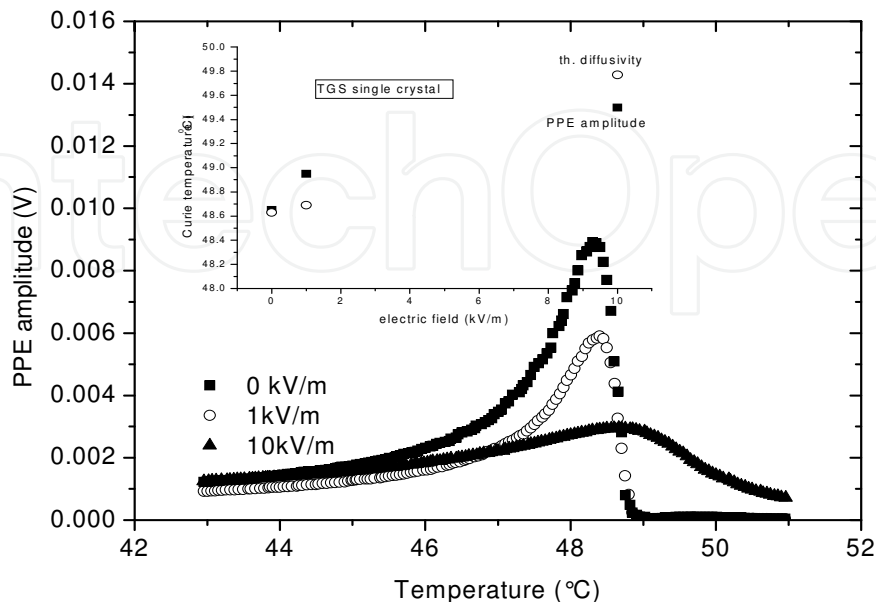

Fig. 4.14 Typical behaviour of the amplitude of the PPE signal for empty TGS sensor and for three values of the external electric field. Insertion: The Curie temperature vs. electric field, as obtained from thermal diffusivity and PPE amplitude (inflection point).

In conclusion to this sub-section, the PPE calorimetry, in the "front" detection configuration, was used to measure the critical behaviour of the thermal diffusivity of TGS single crystal.

In a standard PPE experiment (section 4.3.1) the information on the sample's properties is collected and processed. In this approach, we collect the information on the thermal properties of the pyroelectric sensor itself.

We selected the phase of the PPE signal (and not the amplitude) as source of information due to the well known advantages: the phase is independent on the fluctuations of the incident radiation and the signal to noise ratio is higher than in the case of using the amplitude of the signal. Measurements at two different chopping frequencies and calibration procedures were necessary in order to eliminate the instrumental factors and to obtain a mathematical equation depending on solely one thermal parameter, which is the thermal diffusivity.

The applied external electric field has a typical influence on the critical region of the para-ferroelectric phase transition of TGS: both the Curie temperature and the thickness of the critical region slightly increase with increasing value of the electric field.

The results obtained for the value of the thermal diffusivity of TGS and for the value of the Curie temperatures are in good agreement with data reported in the literature and obtained by other techniques (del Cerro et al., 1987).

Finally, we must emphasize that this configuration speculates the fact that the investigated ferroelectric material is pyroelectric as well. The method was used on a classical TGS crystal, but it appears to be a suitable alternative in studying the thermal properties of the ferroelectric liquid crystals, when the ferroelectric state is imposed by a given layered geometry.

5. Discussions and conclusions

5.1 Comparison with other techniques

It is not possible to perform an exhaustive analysis and comparison of the PPE calorimetry with other types of calorimetry, but some particular advantages of this technique can be mentioned. First of all, due to the fact that the pyroelectric sensor "feels" the temperature variation (and not the temperature), no special thermostatic precautions are requested. This is an advantage compared with adiabatic types of calorimetry, for example. If we compare PPE with differential scanning calorimetry (DSC), PPE is more accurate in detecting the critical temperature (Curie point for ferroelectrics), due to the possibility of scanning very slow (few mK/min – see for example Marinelli et al., 1992) the temperature of the detection cell. In the case of DSC, it is known that the sensitivity increases with increasing temperature variation rate (decreasing the accuracy in measuring the critical temperature).

We cannot overtake two general features that make the PPE calorimetry "unique": (i) it is the only calorimetric technique able to give in one measurement the value of two (in fact all four) thermal parameters; (ii) it is the only technique which, in the critical region of a phase transition, for a given anomaly in the thermal parameters, produces an enhanced signal anomaly.

Finally, some comparison with other PT techniques is welcome. Marinelli et al., 1992 tried to compare the performances of the PPE technique in detecting phase transitions, with another photothermal technique largely used for phase transitions investigations: the photoacoustic (PA) method.

If we follow only the phase channels, they are given in the standard configuration, with optically opaque and thermally thick sample by the equations (Zammit et al., 1988; Marinelli et al., 1992):

$$\Theta_{PA} = \tan^{-1}\left(-1 - 2/p\right); p = \beta_s \left(2\alpha_s / \omega\right)^{1/2} \tag{5.1}$$

for PA phase, and

$$\Theta_{PPE} = -\tan^{-1}\left(\omega\tau_e\right) - 1/q ; \quad q = \left(1/L_s\right)\left(2\alpha_s / \omega\right)^{1/2} \tag{5.2}$$

for PPE phase.

The sensitivity of the two techniques to changes in p and q, respectively, are:

$$\left(\frac{d\Theta}{dp}\right)_{PA} = \left(p^2 + p + 2\right)^{-1} \tag{5.3.a}$$

$$\left(\frac{d\Theta}{dq}\right)_{PPE} = q^{-2} \tag{5.3.b}$$

An analysis of Eqs. (5.3.a,b) leads to the conclusion that the maximum sensitivity of the PA technique is reached when p=0 and has the value ½. In the mean time the sensitivity of the PPE technique can go (at least theoretically) to infinity, denoting once again the suitability of this technique for phase transitions detection.

5.2 General features of the PPE calorimetry

PPE technique is a sensitive and accurate calorimetry for thermal inspection of solid state matter. Concerning ferroelectric materials, the main feature of the method is that two detection configurations can be separately or together used for thermal characterization; the ferroelectric material under investigation can be sample or sensor in the PPE detection cell. All four static (specific heat) and dynamic (thermal conductivity, diffusivity and effusivity) thermal parameters can be measured by this technique, and phenomena associated with changes in time, composition or temperature (phase transitions-for example) can be studied. The sensitivity of the method and the accuracy of the results, when investigating ferroelectric materials, depend on various experimental parameters. The possibility of selecting and adjusting these experimental parameters can lead to an optimization of the performances of the method.

The performances of the method depend practically on: the sensor's detectivity, the precision in monitoring the main experimental parameters (chopping frequency, sample's thickness control, temperature, etc), the quality of the sensor-sample thermal contact, the way of performing the acquisition and processing of experimental data. Some typical experimental data are: the detectivity of the pyroelectric $LiTaO_3$ sensors is higher than 10^8 cm $Hz^{1/2}W^{-1}$; minimum detectable temperature variation: 1 μK; minimum controllable temperature variation rate: 10 mK; frequency stability: 10^{-4} Hz.

The main limitations of the technique concerning ferroelectric materials are imposed by the Curie temperature of the pyroelectric sensor, by the properties of the coupling fluid (always necessary when inserting the ferroelectric material as a sample) and by the geometry of the investigated sample (it must be a disk of tens-hundreds of micrometers thick, with polished surfaces).

6. References

Bentefour E.H., Glorieux C., Chirtoc M. &Thoen J. (2003). Characterization of pyroelectric detectors between 170 and 300 K using the photopyroelectric technique, *Review of Scientific Instruments*, Vol. 74, No. 1,(January 2003), pp. 811-813, ISSN 0034-6748

Bhalla A. S. , Liu S. T. (1993). 4.2.3 Pyroelectric coefficients of ferroelectric pyroelectrics, In *: Electrical Properties - Low Frequency Properties of Dielectric Crystals - Piezoelectric, Pyroelectric, and Related Constants , The Landolt-Börnstein Database* , D.F. Nelson (Ed.), Vol. 29b, Springer Verlag, ISBN 978-3-540-55065-5.

Chirtoc, M., Glorieux, C. & Thoen, J.(2009). Thermophysical Properties and Critical Phenomena Studied by Photopyroelectric (PPE) Method, In: *Thermal Wave Physics and Related Photothermal Techniques: Basic Principles and Recent Developments*, E. M. Moraes, (Ed), 125-159, Transworld Research Network, ISBN 978-81-7895-401-1, Kerala, India

Chirtoc, M. & Mihailescu, G.(1989). Theory of Photopyroelectric Method for Investigation of Optical and Thermal Materials Properties. *Physical Review*, Vol. B40, No. 14, (November 1989), pp. 9606-9617, ISSN 1098-0121

Clark N. and Lagerwall S. T.(1980). Submicrosecond Bistable Electro-Optic Switching in Liquid Crystals. *Applied Physic. Letters.* 36 (1980) pp899-901, ISSN 0003-6951

Coufal, H. (1984). Photothermal Spectroscopy Using a Pyroelectric Thin-Film Detector. *Applied Physics. Letters*, Vol. 44, No. 1, (January 1984), pp.59- 61, ISSN 0003-6951

del Cerro, J., Ramos, S. & Sanchez-Laulhe, J. M. (1987). Flux Calorimeter for Measuring Thermo-physical Properties of Solids: Study of TGS. *Journal of Physics E: Scientific Instruments,* Vol. 20, No. 6, (June 1987), pp. 612-615, ISSN 0957-0233

Delenclos, S., Chirtoc, M., Hadj Sahraoui, A., Kolinsky, C. & Buisine, J. M. (2002). Assessement of Calibration Procedures for Accurate Determination of Thermal Parameters of Liquids and their Temperature Dependence Using the Photopyroelectric Method. *Review of Scientific Instruments*, Vol. 73, No.7, (July 2002), pp.2773-2780, ISSN 0034- 6748

Fullem, T. Z., and Y. Danon, Electrostatics of pyroelectric accelerators. *Journal of Applied Physics* Vol. 106, No 7, (October 2009), ISSN 0021-8979

Jalink, H., Frandas, A., van der Schoor, R. & Bicanic, D. (1996). New Photothermal Cell Equiped with Peltier Elements for Phase Transition Studies. *Review of Scientific Instruments*, Vol. 67, No. 11, (November 1996), pp.3990-3993, ISSN 0034- 6748

Lagerwall S. T., *Ferroelectric and Antiferroelectric Liquid Crystals.* (1999). Wiley-VCH, ISBN 978-3527298310, New York

Mandelis, A. (1984). Frequency Domain Photopyroelectric Spectroscopy of Condensed Phases: A New, Simple and Powerful Spectroscopic Technique. *Chemical Physics Letters*, Vol. 108, No. 4, (July 1984), pp. 388-392, ISSN 0009-2614

Mandelis, A. & Zver, M. M. (1985) J. Theory of Photopyroelectric Effect in Solids. *Journal of Applied Physics,* Vol. 57, No. 9, (May 1985), pp. 4421-4430, ISSN 0021-8979

Mandelis, A., Care, F., Chan, K. K. & Miranda, L. C. M. (1985). Photopyroelectric Detection of Phase Transitions in Solids. *Applied Physics A,* Vol. 38, No. 2, (October 1985), pp. 117-122, ISSN 0947-8396

Marinelli, M., Zammit, U., Mercuri, F. & Pizzoferrato, R.(1992). High Resolution Simultaneous Photothermal Measurements of Thermal Parameters at a Phase Transition with the Photopyroelectric Technique. *Journal of Applied Physics*, Vol. 72, No. 3, (August 1992), pp.1096-1100, ISSN 0021-8979

Nakamura M., Takekawa S & Kitamura K, Anisotropy of thermal conductivities in non- and Mg-doped near-stoichiometric LiTaO3 crystals, *Optical Materials*, Vol. 32, No 11, (September 2010), pp. 1410-1412, ISSN 0925-3467

Tam, A. C. (1986). Applications of Photoacoustic Sensing Techniques. *Review of Modern Physics*, Vol. 58, No. 2, (February 1986), pp. 381-431, ISSN 0034-6861

Zammit, U., Marinelli, M., Mercuri, F.,Pizzoferrato, R., Scudieri, F. & Martelucci, S. Photoacoustics as a Technique for Simultaneous measurement of Thermal Conductivity and Heat Capacity. *Journal of Physics E-Scientific Instruments*, Vol. 21, No. 10, (October 1988), pp.935-941, ISSN 0957-0233

Whatmore R.W., Pyroelectric Devices and Materials, *Reports on Progress in Physics*, Vol. 49 (December 1986), pp1335-1386, ISSN 0034-4885
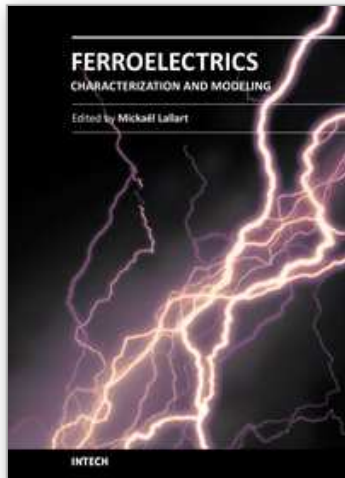
Ferroelectrics - Characterization and Modeling
Edited by Dr. Mickaël Lallart

ISBN 978-953-307-455-9

Hard cover, 586 pages

Publisher InTech

Published online 23, August, 2011

Published in print edition August, 2011

Ferroelectric materials have been and still are widely used in many applications, that have moved from sonar towards breakthrough technologies such as memories or optical devices. This book is a part of a four volume collection (covering material aspects, physical effects, characterization and modeling, and applications) and focuses on the characterization of ferroelectric materials, including structural, electrical and multiphysic aspects, as well as innovative techniques for modeling and predicting the performance of these devices using phenomenological approaches and nonlinear methods. Hence, the aim of this book is to provide an up-to-date review of recent scientific findings and recent advances in the field of ferroelectric system characterization and modeling, allowing a deep understanding of ferroelectricity.

How to reference

In order to correctly reference this scholarly work, feel free to copy and paste the following:

Dadarlat Dorin, Longuemart Stéphane and Hadj Sahraoui Abdelhak (2011). Characterization of Ferroelectric Materials by Photopyroelectric Method, Ferroelectrics - Characterization and Modeling, Dr. Mickaël Lallart (Ed.), ISBN: 978-953-307-455-9, InTech, Available from: http://www.intechopen.com/books/ferroelectrics-characterization-and-modeling/characterization-of-ferroelectric-materials-by-photopyroelectric-method

INTECH
open science | open minds